CMLS, Cell. Mol. Life Sci. 57 (2000) 1909–1926
1420-682X/00/141909-18 $ 1.50 + 0.20/0

CMLS Cellular and Molecular Life Sciences

Review

Ferrochelatase at the millennium: structures, mechanisms and [2Fe-2S] clusters

H. A. Dailey*, T. A. Dailey, C.-K. Wu[1], A. E. Medlock, K.-F. Wang, J. P. Rose and B.-C. Wang

Department of Biochemistry and Molecular Biology, and Department of Microbiology, University of Georgia, Athens (Georgia 30605-7229, USA), Fax + 1 706 542 7567, e-mail: hdailey@arches.uga.edu

Received 17 May 2000; received after revision 28 June 2000; accepted 30 June 2000

Abstract. Ferrochelatase (E.C. 4.99.1.1, protoheme ferrolyase) catalyzes the insertion of ferrous iron into protoporphyrin IX to form protoheme (heme). In the past 2 years, the crystal structures of ferrochelatases from the bacterium *Bacillus subtilis* and human have been determined. These structures along with years of biophysical and kinetic studies have led to a better understanding of the catalytic mechanism of ferrochelatase. At present, the complete DNA sequences of 45 ferrochelatases from procaryotes and eucaryotes are available. These sequences along with direct protein studies reveal that ferrochelatases, while related, vary significantly in amino acid sequence, molecular size, subunit composition, solubility, and the presence or absence of nitric-oxide-sensitive [2Fe-2S] cluster.

Key words. Ferrochelatase; heme synthesis; iron sulfur cluster; metallation; porphyria.

Heme is an almost ubiquitous compound of living organisms, although it is not present in some extremophiles and a few pathogenic bacteria. Interestingly, among heme-containing organisms, only a few are unable to synthesize the compound and instead acquire it from their diet. Biochemical study of the biosynthetic pathway for heme began in earnest in the 1940s and it was not until the 1960s that the last enzyme, the penultimate enzyme in the pathway, was identified. In 1956, Goldberg's group reported the existence of an enzyme activity in avian erythrocytes that catalyzed the insertion of iron into protoporphyrin to form heme [1]. The name given this enzyme was ferrochelatase (protoheme ferrolyase, E.C. 4.99.1.1). In the decade following this initial description, ferrochelatase activity was reported for a variety of cell types and some preliminary kinetic characterizations, mainly from Jones' group [2–4], were published. However, in 1972 [5] and 1973 [6], two independent groups published data suggesting that non-enzymic iron insertion into protoporphyrin occurred in vitro under what they called physiological conditions. While these authors' view of what constituted 'physiological conditions' may be questioned, their data did raised some doubts at the time concerning the need for an enzyme to catalyze this metallation. The authenticity of an enzymatic basis for iron chelation was, however, settled in 1974 with the description of a ferrochelatase-deficient mutant of the bacterium *Spirillum itersonii* that was an auxotroph for heme [7]. Aminolevulinate or protoporphyrin could not substitute for heme, and spontaneous revertants of this mutant regained ferrochelatase activity and no longer required exogeneously supplied heme.

Over the next decade, several attempts to purify the enzyme were reported with final success coming in 1981 when a detergent-solubilized rat liver mitochondrial fer-

* Corresponding author.
[1] Present address: National Cancer Institute, P.O. Box B, Frederick (Maryland 21702, USA).

rochelatase was successfully purified by employing a blue Sepharose column with a variety of salt and detergent washes [8]. While enzyme recoveries with this procedure were reported to be 25%, the small amount of enzyme present in the starting material meant that less than 1 mg of total protein was recovered. Similar yields were later reported from purifications out of bovine liver [9, 10] and yeast [11]. A major breakthrough came with the initial cloning of ferrochelatase from *Saccharomyces cerevisiae* [12] which was quickly followed by the reported cloning of human [13] and murine [14, 15] ferrochelatases. The first expression and purification of recombinant ferrochelatase was from a baculovirus expression of yeast ferrochelatase in 1992 [16], followed by *Escherichia coli* expression of murine normal and protoporphyric ferrochelatases later that same year [17]. Not until 1994, however, were relatively high expression of recombinant human and mouse ferrochelatase obtained [18].

Parallel to the enzymatic studies and cloning efforts, researchers were examining the biomedical side of ferrochelatase, i.e., its role in the human genetic disease erythropoietic protoporphyria [see refs 19, 20]. Advances in the molecular characterization of the protein ferrochelatase and its genomic organization and regulation have been key to understanding the disease. The present review focuses mainly on animal ferrochelatases since more information is currently available on these enzymes. However, because of their interesting enzymatic and physical characteristics, the biochemical diversity of other eucaryotic and procaryotic ferrochelatases is also examined.

Enzyme activity

Ferrochelatase in vivo catalyzes the insertion of ferrous iron into protoporphyrin IX to form protoheme IX (heme) (fig. 1). However, the enzyme is capable of utilizing a variety of metal and porphyrin substrates [see refs 21 and 22 for detailed reviews]. With regard to the porphyrin substrate, a variety of IX isomer porphyrins with substituents at the 2,4 positions on rings A and B that are uncharged and hydroxyethyl or smaller in size are utilized by the enzyme. Interestingly, the XIII isomer of protoporphyrin which has the vinyl group present at the 1,4 positions, as opposed to the 2,4 positions as is found with protoporphyrin IX, has also been reported to serve as a substrate for sheep ferrochelatase [23]. These data suggest that the size and charge of substituents on the A and B rings are more important than the actual position of these groups. In a departure from the animal ferrochelatases findings, ferrochelatase from the bacterium *Rhodobacter sphaeroides* has been reported to utilize the charged porphyrin, 2,4 disulfonic deuteroporphyrin, as a substrate [24]. These data would suggest a difference in active-site residues near the region where the A and B rings dock. In contrast to the allowed variability on the A and B rings, Jackson's group [23] found that for sheep ferrochelatase, the I isomers of mesoporphyrin and proto-

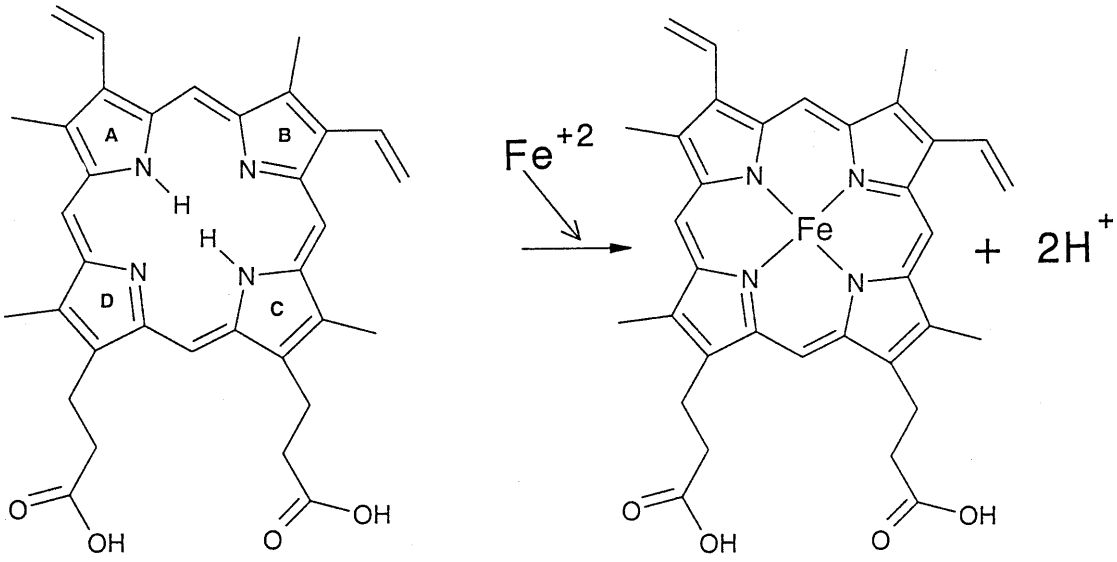

Figure 1. The reaction catalyzed by ferrochelatase. The position of rings A, B, C, and D are shown and the substituent numbering starts with the A ring [i.e. 1 and 2 (A), 3 and 4 (B), 5 and 6 (C), and 7 and 8 (D)].

porphyrin, in which the propionic side chains are in the 6 and 8 positions of rings C and D as opposed to the 6 and 7 positions found in the IX isomers, do not serve as substrates. These data suggest that the absolute positioning of the propionate groups is critical for enzyme catalysis.

Porphyrins that are not substrates may be competitive inhibitors of the enzyme. A variety of IX isomer porphyrins have been examined and those found to be inhibitors had K_is in the range of 13–70 μM, a concentration range similar to the K_ms for substrate porphyrins [25, 26]. Metalloporphyrins containing iron, cobalt, zinc, and tin are also inhibitors with K_is in the 2–13 μM range.

One class of porphyrin inhibitors that deserves particular note are the N-alkyl porphyrins. The history and details of these compounds have been reviewed in detail previously [21] and will only be summarized here. N-alkylprotoporphyrins, which arise in vivo as a result of cytochrome-P450-mediated xenobiotic metabolism, are strong inhibitors of ferrochelatase both in vivo and in vitro. Kinetic analysis shows them to be tight-binding, competitive inhibitors with K_is in the range < 10 nM [9]. The proposed explanation for this low K_i is that these N-alkylporphyrins, which have a distorted macrocycle structure with the alkylated ring tilted about 30° from the planar porphyrin [27, 28], may serve as a transition state analog and are tightly bound by ferrochelatase [21, 29]. A number of kinetic studies have shown that the different alkyl stereoisomers have distinct K_is which must reflect the fact that there is a single preferred orientation of porphyrin in the active site [21, 30, 31]. This suggestion is supported by the recent structure determination of a ferrochelatase-N-methylmesoporphyrin complex in which only a single isomer is found bound in the active site even though the crystal was prepared from an enzyme that had been incubated with a mixture of all possible N-alkyl isomers [32]. Different ferrochelatases have significantly different sensitivities to inhibition by N-alkyl porphyrins, with human ferrochelatase being over 1000-fold more sensitive to inhibition by N-methylprotoporphyrin than is chicken ferrochelatase [33].

Ferrochelatase will catalyze the insertion of a variety of divalent cations, but no monovalent or trivalent metals [see refs 21, 22]. Ferrous iron, cobalt, and zinc are all good substrates for most ferrochelatases although the enzyme from the bacterium *Bacillus subtilis* will not use cobalt, but will use copper. Ferric iron is neither a substrate nor inhibitor of the enzyme. A number of divalent cations are inhibitors of ferrochelatases [34]. Best characterized of these are manganese, cadmium, lead, and mercury. These metals inhibit the enzyme in a competitive fashion with K_is in the range of 10–50 μM, which is comparable to the K_ms for substrate metals.

The role of lead as an inhibitor has attracted some attention since chronic lead exposure in humans results in elevated serum zinc protoporphyrin levels [see refs 19 and 35 and references therein]. At one time lead was thought to inhibit ferrochelatase activity with a resultant accumulation of protoporphyrin. Non-enzymatic zinc chelation would then lead to the observed serum zinc protoporphyrin. While lead clearly does inhibit ferrochelatase, the K_i for Pb is well above that for an earlier pathway enzyme, 5-aminolevulinate dehydratase [36]. Experimental data have been forwarded suggesting that ferrochelatase itself is not inhibited, but that decreased iron availability leads to enzymatic insertion of zinc rather than iron [35]. An additional hypothesis is that lead inhibits the enzyme system which provides reduced iron for ferrochelatase [37]. While interesting, this hypothesis require additional data for verification.

One of the problems associated with ferrochelatase has been the difficulty in assaying the enzyme. In addition to low levels in biological samples, there are three major difficulties: (i) the insolubility of the porphyrin substrate in aqueous solution, (ii) the rapid oxidation of ferrous to ferric iron in the presence of oxygen, and (iii) the photosensitivity of the heme product in the presence of thiol-containing compounds. These problems have long been known [38, 39] and some have even been 'rediscovered' on occasion [40, 41]. Unfortunately, a number of investigations have been published in which incompletely detailed or inappropriate assay procedures have employed resulting in data of questionable value. Attempts to circumvent assay technical problems include carrying out reactions anaerobically, substitution of metal other than iron, such as cobalt or zinc, as substrate, utilization of more soluble porphyrins such as deuteroporphyrin, and doing assays under low-light conditions. A currently popular assay employs zinc and deuteroporphyrin with continuous spectrofluorometric detection. While adequate for screening assays, the use of two non-physiological substrates whose chemical properties are quite distinct from those of the physiological substrates, iron and protoporphyrin, makes this assay unacceptable for serious kinetic characterization of both normal and mutant forms of ferrochelatase.

One of the most common assays of ferrochelatase uses physiological substrates with product quantitation of the pyridine hemochromogen [38, 39]. This assay system, while useful, must be employed with proper caution since thiol compounds frequently included in the assay mixture will catalyze the photodestruction of the pyridine hemochromogen if they are not dealt with. Another older technique that has seldom been employed of late is the 'dual-wavelength' assay [38]. This assay takes advantage of the spectral shift that occurs upon metal insertion and, depending upon available equipment, can be used to monitor enzyme activity

continuously. This assay system apparently failed to find broad acceptability because the sensitivity is significantly less than either the pyridine hemochromogen or zinc/deuteroporphyrin fluorescence methods of detection. With the recent availability of larger quantities of pure ferrochelatase and spectrophotometers with greater sensitivity and reliability, this assay may become the one of choice.

Diversity and ferrochelatase evolution

Ferrochelatase activity similar in nature to that first described in avian erythrocytes [1] has been widely found in bacteria and eucaryotes. At the time of writing, 45 complete ferrochelatase cDNA or DNA sequences were present in GenBank and TIGR databases, although few ferrochelatases have actually been expressed and characterized. However, ferrochelatase has not yet been reported in any Archae including those known to synthesize heme.

One possible explanation for this is that typical ferrochelatases exist in this kingdom but their sequences are too dissimilar to other known ferrochelatases to be identified by a homology comparison search. A second possibility is that a totally different mechanism exists for metallation of porphyrins in the Archae. Arguments in support of this second possibility would be based upon the observation that cobalt chelatase, which inserts cobalt into a corrin macrocyle for vitamin B_{12} biosynthesis in *Pseudomonas denitrificans*, has been shown to be a multisubunit ATP-requiring enzyme [42]. This cobalto-chelatase has one subunit, CobN, which binds corrin and cobalt, and is similar to BchH of magnesium chelatase. The CobS protein shows similarity to BchI of magnesium chelatase, but the CobT protein shows no homology to BchD of magnesium chelatase. Genome comparison has suggested that the nickel chelatase of *Methanococcus jannaschii*, which must exist for F430 synthesis, may also be a magnesium chelatase homolog [43]. Thus, it would not be surprise if the Archae, which possess a rich array of metal tetrapyrrole-type compounds, have evolved similar solutions for all metal-chelatase-requiring reactions. One cautionary note, however, is that a cobalto-chelatase from *Salmonella typhimurium* has strong structural similarities to ferrochelatase of *B subtilis* [44], but this protein lacks sufficient sequence similarity to be identified as a protein homolog of ferrochelatase even though the structural comparisons make this relationship clear. A similar example may be the CysG gene product that encodes a sirochlorin ferrochelatase for siroheme synthesis [45]. Thus, lack of an identifiable ferrochelatase sequence in the Archae does not rule out the possibility of its existence.

Phylogenetic analysis of the protein sequences results in the clear segregation of animal and plant ferrochelatases (fig. 2). However, procaryotic ferrochelatases do not cluster into a single grouping. Perhaps surprising is that even the bacterial enzymes possessing carboxyl-terminal extensions (see below) do not cluster together and *Aquifex aeolicus*, which is the most ancient of the bacteria listed in this analysis, has a ferrochelatase that clusters more closely with eucaryotes and [2Fe-2S]-cluster-containing bacteria than it does with most bacteria even though it does not possess a carboxyl-terminal extension.

Among all currently known ferrochelatases there is only 5% identity among the 330 core residues that all of these enzymes possess and less than 15% highly conserved residues. Human and *B. subtilis*, the two best characterized ferrochelatases, have only 7% identity but these proteins are clearly closely related (fig. 3). However, sequence comparison reveals two major differences. One of these is the presence of an amino-terminal signal sequence in human and all eucaryotes which is responsible for targeting the enzyme to mitochondria and/or chloroplasts. This region is lacking in bacteria where such translocation does not occur. The second clear difference is the presence of a carboxyl-terminal extension in all eucaryotes that is lacking in a majority of currently identified procaryotic ferrochelatases. By comparison with *B. subtilis* or *E. coli* ferrochelatases, all eucaryotic ferrochelatases possess additional carboxyl-terminal amino acid residues. The length of this extension is typically 30 residues in yeast and animals and approximately 50 residues in plants.

All bacteria were originally suggested to lack this region, but more recently, a number of bacteria, including *Caulobacter*, *Rickettesia*, *Mycobacterium*, *Streptomyces*, and *Propiobacterium*, have been found to possess a carboxyl-terminal extension. Interestingly, the sequences of these carboxyl-terminal extensions have no similarity to those of eucaryotes and little similarity to one another. Alignment programs such as ClustalW will align the carboxyl 30 residues of all animal ferrochelatases, but cannot align any of the bacterial sequences with the eucaryotic animal sequences. Visual alignment of just the bacterial sequences results in pairing of *Caulobacter* with *Rickettesia*, *Streptomyces* with *Propionibacterium*, and the *Mycobacteria* as a separate group. Close examination of these bacterial sequences reveals that *Caulobacter* and *Rickettesia* share a similar three-cysteine motif (C-X_6-C-X-C) in this region, *Streptomyces* and *Propionibacterium* possess a different three-cysteine motif (C-X_3-C-C), and *Mycobacterium* possesses yet another three-cysteine motif (C-X_8-C-X_4-C). We have found that all three groups of these bacteria also possess [2Fe-2S) clusters, but that these clusters have properties that are distinct from those of animal

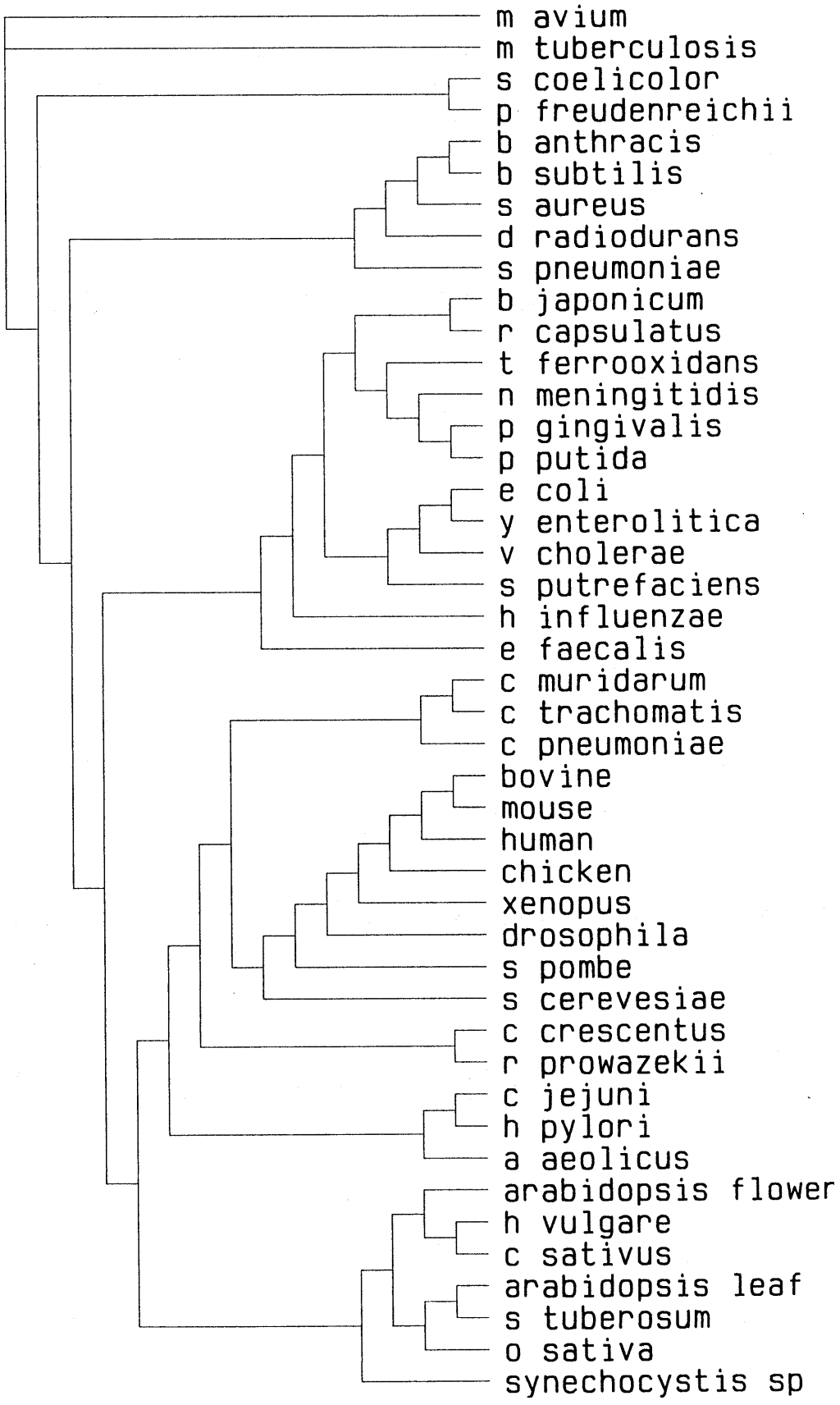

Figure 2. PAUP protein cladogram of currently known ferrochelatases. The protein sequences obtained from GenBank and TIGR databases were subjected to the Paupdisplay Cladogram program.

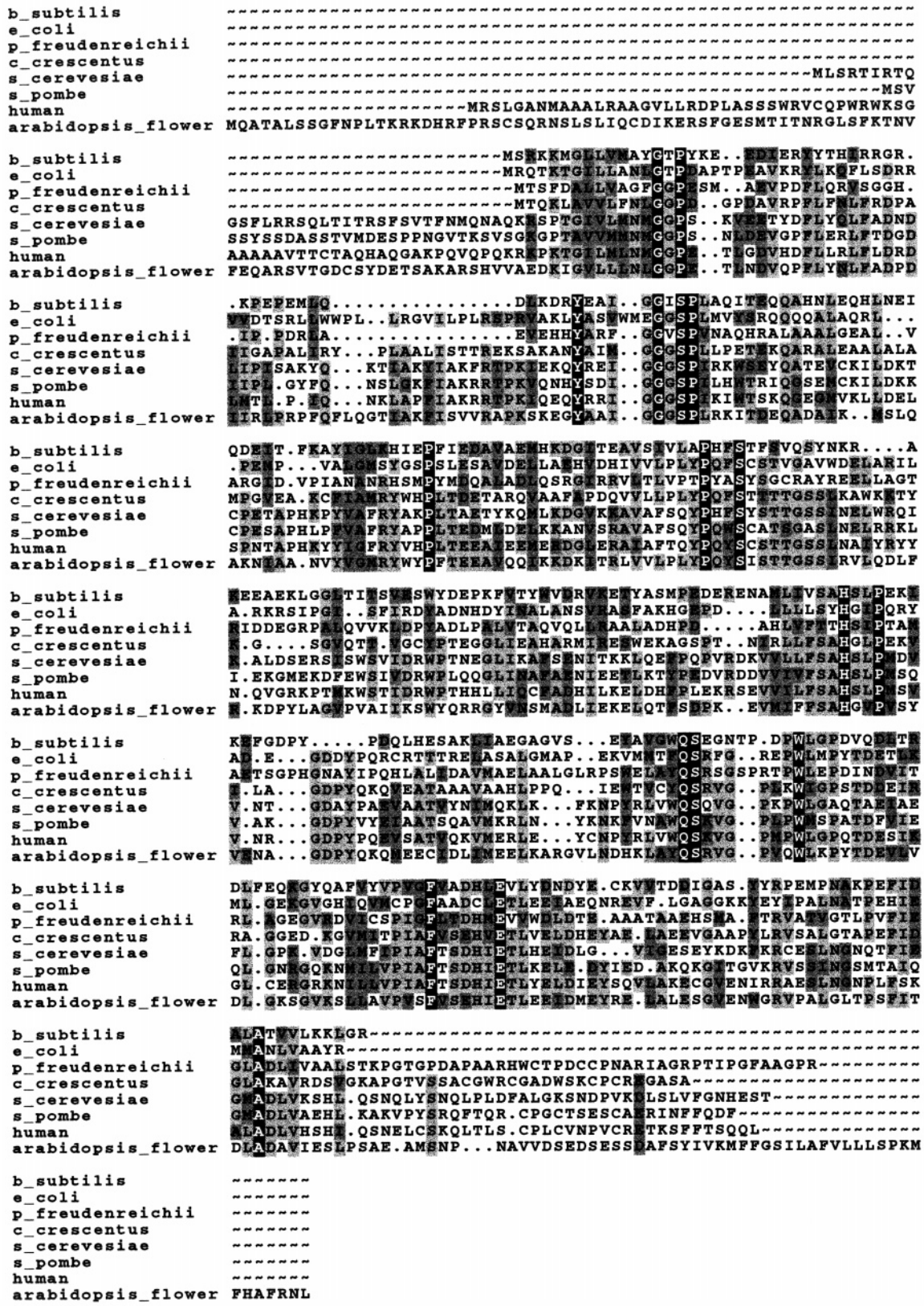

Figure 3. Pileup of selected ferrochelatase sequences. The sequences in the figure present examples of monomeric, dimeric, soluble, and membrane-associated ferrochelatases (see text). Box shading denotes residues that are identical among all these selected sequences (black) and residues that are conserved (grey).

ferrochelatase [2Fe-2S] clusters [H. A. Dailey and T. A. Dailey, unpublished data; H. A. Dailey et al., unpublished data].

Considerable diversity exists among bacterial ferrochelatases. As mentioned above, the enzyme from *B. subtilis* is a water-soluble monomer. Membrane attachment of human ferrochelatase is believed to be mediated in part via a 12-residue extension on one of the active-site lips which is lacking in the *B. subtilis* enzyme (see below). Assuming that this membrane attachment hypothesis is correct, then by sequence comparison, *Bacillus*, *Deinococcus*, *Staphylococcus*, *Mycobacterium*, *Propionibacterium*, *Streptomyces*, and *Streptococcus* ferrochelatases are expected to be soluble proteins since they all lack this 12-residue feature in their sequences.

Another difference between human and *B. subtilis* ferrochelatases is that the human protein is a homodimer while the bacterial enzyme is monomeric. From the crystal structure, the dimerization motif of the human ferrochelatase is clearly the carboxyl-terminal extension (see below). Elimination of this segment would make dimerization impossible and thus the *B. subtilis* enzyme which lacks this feature is monomeric. If one assumes that proteins lacking the carboxyl-terminal extension are monomeric and those possessing the extension are dimeric, then the enzymes from *Streptomyces*, *Propionibacterium*, and *Mycobacterium* would be expected to be soluble dimers, those from *Caulobacter* and *Rickettsia* would be membrane-associated dimers, those from *Streptococcus*, *Deinococcus*, and *Staphylococcus* would be soluble monomers, and in all other currently known bacteria, such as *E. coli*, *Yersinia*, *Bradyrhizobium*, *Haemophilus*, *Rhodobacter*, *Vibrio*, *Helicobacter*, and *A. aeolicus*, they would be membrane-associated monomers.

While there is still little hard data available for all of these bacterial ferrochelatases, there is one item of interest. *B. subtilis*, the preceding pathway enzyme, protoporphyrinogen oxidase (PPO), is a soluble monomer as is the ferrochelatase of that bacterium. In *A. aeolicus*, both PPO and ferrochelatase are membrane-associated monomers [K.-F. Wang and H. A. Dailey, unpublished data]. Some bacteria, such as *Myxococcus xanthus*, possess a membrane-associated dimeric PPO as is found in animal PPOs. These limited observations lead to the speculation that the oligomeric state and solubility of ferrochelatase and PPO are linked within an organism. This pattern, should it prove to be accurate and universal, is intriguing and suggests that these two enzymes may exist in situ in a functional complex. The nature of such a complex will be interesting to describe since the cellular compartments in which these enzymes are located vary between eucaryotes and procaryotes. In eucaryotes, a trans-membrane complex would have to exist since the two enzymes are located on opposite sides of the mitochondrial inner membrane [22, 46, 47], whereas in bacteria with membrane-associated PPO and ferrochelatase, both enzymes are anticipated to be on a common surface of the cytoplasmic membrane although the exact localization and sidedness of these enzymes has never been reported for any bacterium. Thus, the interacting surface versus membrane-associating surface would be expected to vary between eucaryotes and procaryotes. For soluble PPO and ferrochelatase, there is no membrane-associating surface, so the site of protein-protein contact is not restricted. While it would be expected to be close to face-to-face for ready transfer of the tetrapyrrole substrate, flexibility would be needed to allow product dissociation to occur since there is no evidence from the *B. subtilis* ferrochelatase structure for separate porphyrin entrance and heme exit sites.

Enzyme mechanism

Since ferrochelatase binds a planar macrocyclic porphyrin as substrate and must release a planar macrocyclic porphyrin with an iron inserted, the protein must either have a mechanism to distinguish between these two macrocycles, or bind both substrate and product poorly enough that the product will not remain bound to the enzyme following catalysis. The observations that the K_m and K_i for protoporphyrin and protoheme are similar (micromolar) and that enzyme turnover as measured in vitro is quite low (on the order of 10 min^{-1}) may be consistent with an enzyme that has little ability to differentiate between porphyrin substrate and product. This may be acceptable in vivo where cellular processes exist to efficiently and rapidly utilize any product formed and to limit substrate availability.

The mechanism whereby ferrochelatase inserts iron into the porphyrin has been discussed previously [21, 22, 29] with the general consensus that macrocycle distortion is the most probable and thermodynamically favorable process. Support for this model comes from a variety of approaches including non-enzymatic solution studies [48], kinetic studies of the enzyme, characterization of metallation by catalytic antibodies [49], catalytic DNAs [50] and RNAs [51], and resonance Raman spectroscopic studies of both ferrochelatase and catalytic antibodies [52–54]. These last studies revealed that ferrochelatase binds porphyrin and distorts it into a domed [52] or ruffled [54] conformation. Interestingly, this distortion was only seen when a metal ion was bound to the yeast enzyme [52] although porphyrin binding with distortion by the mouse enzyme was found to occur in the absence of metal ion [54]. The crystal structure of *B. subtilis* ferrochelatase with bound N-methylmesoporphyrin has been reported and clearly shows that the distorted macrocycle is tightly bound in the enzyme active site [33].

Taken as a whole, the various pieces of data now available very strongly support a role for macrocycle distortion as a step in ferrochelatase-catalyzed metallation. Whether this involves doming of the entire molecule, or distortion of a single pyrrole ring of the macrocycle is presently not clear. Since the resonance Raman studies with the yeast enzyme involved a metabolizable porphyrin with a non-metabolizable metal substrate, the corresponding studies with mouse ferrochelatase did not examine an arrested complex, and the crystallographic studies with *B. subtilis* ferrochelatase employed a non-metabolizable porphyrin substrate, if actual catalysis requires doming, or if a single ring distortion is sufficient is not clear. Answers to this question may come from examination of mutant forms of the enzyme that form arrested, stable transition state complexes.

Studies of non-enzymatic porphyrin metallation strongly suggest that the incoming metal forms a 'sitting-atop complex' on the porphyrin macrocycle and inserts into the distorted porphyrin as the pyrrole protons exit from the opposite side [44, 48]. Data do not support a stepwise deprotonation of the porphyrin followed by metallation which would be required if deprotonation and metallation both occur on the same side of the macrocycle. Since enzymatic metallation is anticipated to follow the same general process as solution chemical metallation, the active site of ferrochelatase would possess residues on one side of the pocket dedicated to metal binding and residues on the opposite side of the pocket involved in proton abstraction.

Eucaryotic ferrochelatases

Eucaryotic ferrochelatases are nuclear encoded and synthesized in the cytoplasm as a pre-protein with an amino-terminal, organellar targeting sequence [55]. Plants apparently produce two ferrochelatases, one targeted to mitochondria and one to chloroplasts [56]. Suzuki et al. [57] have presented evidence that in cucumber there may be tissue specificity with different ferrochelatases for photosynthetic and non-photosynthetic tissues. In non-plant eucaryotes, a single ferrochelatase is synthesized and it possesses a leader sequence that targets the precursor protein to the matrix side of the inner mitochondrial membrane [4, 55, 58]. Following a membrane potential requiring translocation into the mitochondrial matrix, proteolytic processing converts the protein into its mature form. Mature eucaryotic ferrochelatases are membrane-associated proteins that do not possess any membrane-spanning segments. The molecular weight of the mature, processed animal enzyme polypeptide is approximately 42 kDa. The plant enzyme is slightly larger with approximately 20 additional amino acid residues present at the carboxy terminus.

Crystal structure

The crystal structure of human ferrochelatase has now been solved to 2.0 Å [59]. This refined structure contains essentially all of the residues of the mature protein (residues 62–423) and has excellent density for all side chains (fig. 4A). This enzyme is a homodimer of 86 K, which is in agreement with radiation inactivation studies [60] and dynamic light-scattering measurements [61]. The individual subunits of human ferrochelatase have resemblance to the gross structure of *B. subtilis* ferrochelatase [62]. The structure contains approximately 48% α helix and 14% β sheet. Each monomer is comprised of two similar domains in a motif resembling that found in the periplasmic-binding protein family. Two significant deviations between the two domains are an additional N-terminal loop (residues 95–104), and a C-terminal extension (residues 390–423). The N-terminal loop comprises part of the one 'lip' of the active-site pocket and the C-terminal extension is involved in coordination of the [2Fe-2S] cluster and dimer stabilization.

Although human ferrochelatase is a homodimer, the *B. subtilis* enzyme is monomer [62]. The explanation for this becomes clear from examination of the crystal structures of the two enzymes. The dimer interface of human ferrochelatase is stabilized by 30 hydrogen bonds, 18 of which are associated with the carboxyl-terminal 30 residues present in eucaryotic ferrochelatases. Thus, this region may be viewed, at least in part, as a dimerization motif for ferrochelatase. *B. subtilis* ferrochelatase, however, is monomeric because it lacks the necessary carboxyl-terminal segment that is essential to stabilize the dimer. The role dimerization may play is unknown at present, but it is of note that elimination of the carboxyl-terminal extension in eucaryotic ferrochelatases results in loss of enzyme activity [18, 63].

Each subunit of human ferrochelatase contains a deep, but open, active-site pocket as was predicted by earlier spectroscopic studies [64]. In the homodimer, both active-site pockets are located on a single surface of the molecule (fig. 4B). The opening of each active-site pocket consists of two hydrophobic lips composed of residues 300–311 and 90–130 (fig. 5A). The inner surface of one lip contains R114 and R115 which may be involved in interactions with one propionate side chain of the porphyrin substrate [65]. The external sides of these lips are rich in hydrophobic residues, the result being that the active-site-containing surface of the homodimer is the largest non-polar molecular surface. Compared to the lips, the active-site pocket is relatively hydrophilic and contains most of the highly conserved

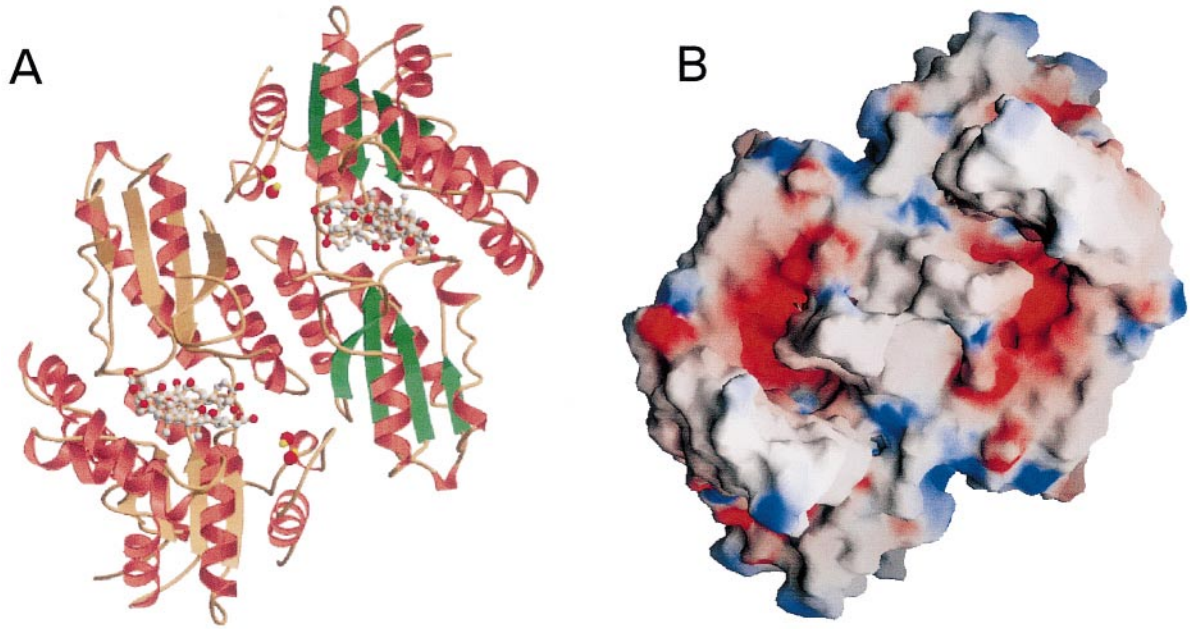

Figure 4. Crystal structure of homodimeric human ferrochelatase. (*A*) Ribbon drawing of human ferrochelatase. The figure was prepared with MOLSCRIPT and is of the homodimer. The [2Fe-2S] clusters are present in the dimer interface and the position of the two active sites can be determined by the presence of the cholate detergent molecules which are present in the crystallized protein. (*B*) The electronic surface potential of human ferrochelatase as modeled by GRASP. In this orientation, the active sites and protruding hydrophobic (white) lips face the viewer. The lip regions surrounding the pockets form the largest hydrophobic patch on the protein surface. This region is suggested to associate with the matrix side of the inner mitochondrial membrane in vivo. The interiors of the active-site pockets are highly hydrophilic and the residues visible from this angle are largely acidic (red). Basic regions are colored blue.

residues. A significant structural variation between the membrane-associated human ferrochelatase and the water-soluble *B. subtilis* enzyme is a 12-residue N-terminal α-helical insertion found in the lip region of the human protein [59]. Based upon sequence comparisons, this region has been previously hypothesized to be involved in membrane association [66]. This was supported by the human enzyme crystal structure which demonstrates that this lip region is detergent associated and contributes to a largely hydrophobic surface that is not found on the *B. subtilis* enzyme [59]. In the intact enzyme, this hydrophobic surface is expanded due to the two-fold symmetry of the dimer and also serves to position both active-site pockets on the same hydrophobic surface.

This finding is of interest for two reasons. First, the substrate, protoporphyrin IX, and product, protoheme IX, are both poorly soluble in aqueous environments at neutral pH. Positioning the active sites towards the hydrophobic membrane would allow substrate and product to enter and leave via the membrane thereby eliminating the need to partition substrate and product into the aqueous mitochondrial matrix. In addition, PPO, the preceding enzyme in the pathway, is membrane associated and located across the inner mitochondrial membrane from ferrochelatase [46]. Such an arrangement would favor rapid product/substrate exchange and may give support for a transmembrane complex of these two proteins as has been suggested previously [21, 46, 47].

The [2Fe-2S] cluster

All animal ferrochelatases examined to date possess a [2Fe-2S] cluster [18, 67–70]. The crystal structure of the human enzyme confirmed the presence of one cluster per monomer (fig. 4A) and the unusual Cys-X_{206}-Cys-X_2-Cys-X_4-Cys coordinating motif that was proposed from site-directed mutagenesis and spectroscopic studies [67, 70, 71]. The human ferrochelatase [2Fe-2S] cluster exhibits a number of interesting features. Unlike most [2Fe-2S] clusters that show additional hydrogen bonding to the iron or sulfur atoms, this cluster is only bonded by the ligating cysteine (C196, C403, C406, and C411) residues with no additional hydrogen bonds [59]. Both [2Fe-2S] clusters are located at the dimer interface and are accessible to solvent. In each subunit, the cluster is located approximately 15 Å from the center of the

active-site pocket, but is physically separated from this pocket by the side chains of a few residues.

The measured mid-point potential of -450 mV [61] and the electron paramagnetic resonance signal of the clusters are not unusual [67], but the sensitivity to nitric oxide (NO) [72] and some of the spectroscopic properties are distinct from other currently characterized [2Fe-2S] clusters [71]. The spatial orientation, surrounding environment, and dihedral bond angles for the coordinating cysteine residues of the [2Fe-2S] cluster are of particular interest since the resonance Raman and variable-temperature magnetic circular dichroism measurements for this protein differ from currently known and structurally characterized [2Fe-2S] clusters [67, 71].

The role of the cluster in ferrochelatase is still not defined. Studies with chimeric ferrochelatases constructed from human and yeast ferrochelatases show clearly that enzyme activity is not strictly dependent upon the presence of the cluster [73]. Likewise, the iron of the cluster does not serve as substrate iron in the enzyme reaction. The NO sensitivity of the cluster and the initial finding of this feature in mammalian ferrochelatases led to the suggestion that the cluster might be involved in an immune response [72]. However, the recent finding of the cluster in the yeast *Schizosaccharomyces pombe* and some bacterial ferrochelatases casts doubt upon this hypothesis. The cluster may play some structural role, but the minor contribution made to the protein structure by this feature suggests that other hypotheses should be considered. A role as an 'iron regulatory element' where active enzyme is not assembled in the absence of sufficient iron supply could be considered, but lacks compelling backing with the discovery of the cluster in bacteria. The finding of the cluster in few bacterial ferrochelatases may have eliminated some theories, but emphasize that nature views this feature as significant enough for it to have 'evolved' at least three different times for different organisms (see above). Thus, a definitive and important role is anticipated, but has so far eluded us, probably due to the manner in which the enzyme is assayed in vitro. Still unexamined is the possibility that the redox state of the cluster may have a subtle effect upon enzyme catalysis, or that the cluster serves a protective role to prevent ferrous iron oxidation in situ much as has been suggested for the tightly bound NADPH of mammalian catalase [74].

Structure-based mechanism

Identification of the roles of specific amino acid side chains in catalysis remains to be detailed, but the availability of the crystal structure and results from site-directed mutagenesis of the protein are beginning to

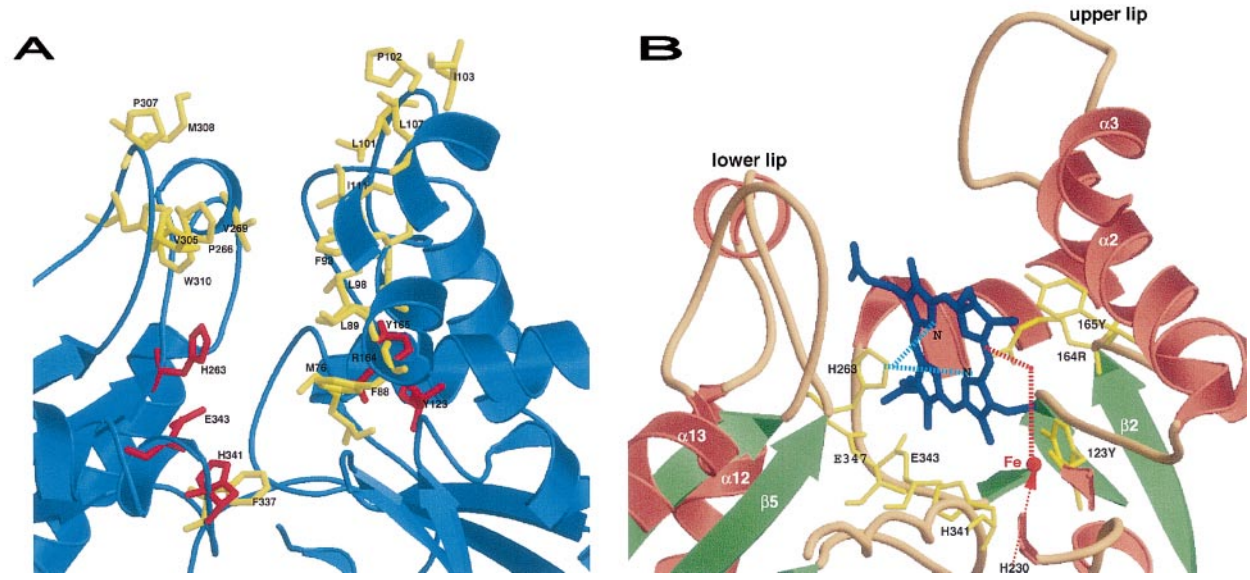

Figure 5. The active site of human ferrochelatase. (*A*) Ribbon diagram of selected residues that line the walls of the pockert. Residues in red are those suggested to be involved in proton abstraction and metallation. Residues in yellow are hydrophobic residues that line the lips of the active site. (*B*) An active-site model for human ferrochelatase. Details of the model are given in the text. The position of the tetrapyrrole is modeled into the pocket based upon the position of detergent molecules found in the crystal structure of human ferrochelatase [59] and the position of N-methylmesoporphyrin in the crystal structure of the *B. subtilis* ferrochelatase [32]. Residues suggested to be involved in catalysis are shown in stick figures on the ribbon backbone structure.

yield some clues. Findings show clearly that residues must participate in substrate ferrous iron binding, porphyrin proton abstraction, porphyrin binding, and ring distortion.

Several key features within the active-site pocket are clearly related to enzyme catalysis. The importance of residue H263 (human numbering) has been identified in a number of studies [53, 54, 62]. This residue is centrally located on the lower lip side of the pocket (fig. 5) and its proper spatial orientation may be stabilized by a hydrogen bond with the conserved Y276 [62]. H263 and its corresponding residue in the yeast [54] and *B. subtilis* [32, 62] enzyme has been suggested to be involved in substrate iron binding. This suggestion has been based largely upon the report by Kohno et al. [75] that site-directed mutagenesis of this residue alters the K_m of the enzyme for iron. We have recently reexamined this proposal by extensive site-directed mutagenesis experiments and find that neither the H263A reported earlier [75] nor H263C/N/M mutations yield active enzyme and no H263 mutant is able to complement a ferrochelatase-deficient strain of *E. coli* (*Δ*hemH) [unpublished data]. The earlier data [75] may have been in error because those investigators employed crude cell extracts of *E. coli* that contained the plasmid-encoded H263A human ferrochelatase rather than purified enzyme. Mutation of the corresponding histidyl residue in yeast ferrochelatase (H235) was reported to be 'practically inactive' when expressed in yeast and could not support the growth of the ferrochelatase-deficient yeast strain *Δ*hem15 in the absence of heme supplementation [76]. Interestingly, when this mutated enzyme was expressed in *E. coli*, the soluble cell fractions had activity, but with 4-fold decreased V_{max}, 8-fold increased K_m for porphyrin, and 290-fold increased K_m for zinc. No attempt to complement the *Δ*hemH mutant of *E. coli* with this enzyme was reported. Taken together, these data along with the 'sitting-atop complex' discussed above cast doubt on the proposed substrate iron binding role for H263 and suggest that this residue serves another key function.

Adjacent to H263 on the same side of the pocket is the highly conserved carboxylate-rich patch composed of D340, H341, E343, and E347 (fig. 5B). These residues form an anionic pathway from H263 in the pocket interior to the outer surface of the protein. Involvement of these residues in proton abstraction [22, 76, 77] and substrate iron supply [76] has been suggested. The available experimental data are consistent with these carboxylate side chains serving in proton abstraction, but not with a role in iron binding/attraction [59; V. M. Sellers et al., unpublished data]. Furthermore, both the abstraction of pyrrole protons and metallation with iron via H263 and these carboxylates would require the formation and temporary stabilization of the dehydroporphyrin in anticipation of iron acquisition and insertion. This appears unlikely and is inconsistent with enzyme kinetic data [9]. Histidyl residues frequently serve a catalytic role as proton acceptors or donors for enzymes, and carboxylates have been shown to participate in proton movement in proteins [78, 79]. Thus, it seems reasonable that H263 initially accepts the pyrrolic protons, and then D340, H341, and E343 participate in a concerted fashion to remove and shuttle the two protons to the external medium.

Recently, Lecerof et al. [32] published the structure of *B. subtilis* ferrochelatase with N-methylmesoporphyrin bound in the active site. Their data clearly demonstrate the orientation of the distorted macrocycle in the active site with the center of the porphyrin ring positioned directly over the equivalent of human H263. Soaking the crystal complex with copper (II) resulted in the demethylation of the alkylated porphyrin and insertion of copper into the distorted macrocycle. Soaking with zinc, another non-physiological metal substrate for the enzyme, did not result in either demethylation or metal insertion. While these authors suggested from these data that normal metallation occurs from H263 and may involve the adjacent carboxylate residues, we would suggest an alternative explanation.

Since the available kinetic data from mutants of the carboxylate-rich region are not consistent with a role for these side chains in iron binding [59], and because demethylation with the *B. subtilis* enzyme occurs without macrocycle planarization, copper may adventiously bind to the enzyme complex and migrate to the available histidyl residue where it reacts with the alkylated porphyrin, catalyzing the demethylation. Two additional pieces of data are also of significance with regard to the previously proposed mechanism of metallation from H263. One is that neither demethylation, nor metal binding, were observed with zinc, and the other is that metallation pathway that involves only this portion of the active site cannot account for the difference in metal specificity seen with the *B. subtitlis* ferrochelatase versus other characterized ferrochelatases.

If H263 is not involved in metallation, then which are the iron-binding residues? From the crystal structure of human ferrochelatase, a number of residues are available as potential substrate iron ligands. Highly conserved residues in the active-site pocket include Y123, Y165, R164, and Y191 (table 1). Mutation of any of these residues in human ferrochelatase altered the K_m for iron without a change for porphyrin as would be expected for residues involved in substrate iron binding [59; V. M. Sellers et al., unpublished data]. The adjacent residues R164 and Y165 are directly opposite H263 which would allow the generation of a 'sitting-atop complex' for metallation (fig. 5B). Lavallee [29] has previously proposed that the ferrous iron ligands of

Table 1. Conserved amino acid residues of ferrochlatase.

Identical residues		Highly conserved residues			
G77	Q302	V85	P168	V287	E347
P79	S303	F88	M177	W301	I348
D95*	W310	L89	P192	G306	L381
R115*	L311	L107*	S195	L311	V385
Y123	P313	I111*	W227	D316	
S130	F337	I132	I241	P334	
P131	E343	G127	S261	D340	
H263		G128	L265	I342	
P266		R164	G273	T344	
Y276		Y165	D274	L345	

The numbering is for human ferrochelatase. This analysis is based upon 44 eucaryotic and procaryotic ferrochelatase sequences in public databases. Identical residues are those that occur in over 95% of the sequences. Highly conserved residues are those with conservative replacements in over 95% of sequences.
* These residues are identical or highly conserved in ferrochelatases that possess this protein segment.

ferrochelatase should include a good Lewis base, and R164 in human may serve that role. Of note is that ferrochelatase of *B. subtilis*, which does not use Co^{2+} as does human ferrochelatase, but will use Cu^{2+} instead, is one of very few ferrochelatases that does not possess the equivalent of R164, Y165 and Y191. Instead, it has K87 (human 164), H88 (human 165), and A114 (human 191).

Y191 is located at the bottom of the active-site pocket and appears too distant to be involved in the actual metallation reaction. Likewise, Y123, which is on the same side of the pocket as R164 and Y165, is spatially too distant to simultaneously participate in the coordination of iron unless there is significant molecular movement. Interestingly, in the human ferrochelatase crystal structure, Y123 was found to be one of several residues involved in ligation of a Ni^{2+} atom [58] which was not displaced by soaking the crystal with Co^{2+}. In a similar position in the *B. subtilis* ferrochelatase structure, a Mg^{2+} atom is found [62], and in the *S. typhimurium* cobalt chelatase, a sulfate ion [80] is located here. The role these metals may play in structure and/or catalysis is not known at present.

The entry site of the metal substrate may differ from that taken by the porphyrin. H230 and D383 were identified in the crystal structure of human ferrochelatase as ligands for exogeneously supplied cobalt, thereby suggesting that this site may represent the initial binding site for substrate iron [59]. Since this site is located on the back side of the enzyme approximately 24 Å from H263 in the center of the active site, additional residues would be needed to move iron into the active site. The conserved residues W227, Y191, R164, and Y165 span the region from H230 into the active site suggesting that W227 and Y191 may be involved in iron translocation into the active site. Additional data are needed to confirm whether H230/D383 is the substrate metal acquisition site, but this model would be consistent with a previous suggestion that iron for heme synthesis in yeast is linked to a specific mitochondrial transport system which may interact directly with ferrochelatase [81].

The nature of the residues involved in porphyrin binding and ring distortion for eucaryotic ferrochelatase are currently not defined. The crystal structure and kinetic data for the human enzyme and several mutants suggest a role for F110 in porphyrin acquisition and/or heme elimination [H. A. Dailey et al., unpublished data]. This residue, which is on one of the active-site lips, would be located within the membrane milieu and crystal data show that it possesses the most mobile side chain in the protein crystal [59]. Mutations at this site result in an enzyme that has activity, but binds heme more tightly than the wild-type enzyme. Within the active site, F337 is a conserved residue whose position is rotated 90° in the inactive mutants of H263 [unpublished data]. This residue, which is located in close proximity to H263, conceivably participates in prophyrin ring distortion since its aromatic side chain is clearly motile and occupies a spatial position that would seem appropriate for such a role.

Considerably more is known about the active site of the *B. subtilis* enzyme since the recent publication of the N-methylmesoporphyrin-ferrochelatase complex structure [32]. In this enzyme, the B, C, and D rings of the alkylated porphyrin, and presumably normal substrate porphyrin, are held tightly in the active site and the A ring is 'bent' by interaction with Y13 and L43. Since these two residues are not conserved in eucaryotic ferrochelatases, and because the overall geometries of the active site of the active of the human and *B. subtilis* enzymes differ considerably with the additional 12 residues on one lip of the human enzyme, direct comparisons are not possible. Indeed, the position of key residues is different enough that mediation of ring binding and distortion via different residues in eucaryotic ferrochelatases would not be unexpected.

Based upon the crystal structure of human and *B. subtilis* enzymes and site-directed mutagenesis studies for human ferrochelatase, the catalytic model initially proposed by Lavallee [29] over a decade ago still appears to best fit all available data. In this model, porphyrin ring binding and distortion may be mediated by conserved hydrophobic and aromatic residues (e.g., Y13 and L43 of the *B. subtilis* enzyme and F337 and other residues in the human enzyme). Proton abstraction occurs from the surface of the porphyrin in proximity to H263, with E343, H341, and E347 forming a pathway for proton movement away from H263. Iron entry may be facilitated via a chain of conserved residues located

on the opposite side of the pocket from H263. Final metallation may then occur from the highly conserved residues of R164 and Y165 (fig. 5B). Access to the active site for the two substrates may occur from distinct routes in the eucaryotic enzyme with porphyrin entering from the membrane-facing surface [24] and iron approaching from a surface of the molecule that is separate from the membrane surface proper. It should be noted that this model may be general only for mitochondrial-associated eucaryotic ferrochelatases since the spatial orientation of ferrochelatase within procaryotic cells may differ, especially for the soluble ferrochelatases, found in *B. subtilis*.

Genomic organization and regulation of mammalian ferrochelatase

Shortly after the isolation of human and murine cDNAs for ferrochelatase, the gene for human ferrochelatase was located to chromosome 18q21.3 [17, 82] and its sequence published [13]. The human ferrochelatase gene is composed of 11 exons covering a region of approximately 45 kb. Exon 1 contains both 5′ untranslated sequence as well as the proposed first 22 amino-terminal residues. It should be noted that no experimental data exist to show that the currently assigned first methionine is the actual translational start. This putative initiation codon does not adhere to the Kozak initiation sequence rules, whereas the second ATG (codon no. 8 in the current sequence) possesses all attributes one expects to find in an initiation codon. Interestingly, the putative first methionine of human and mouse is lacking in bovine ferrochelatase. Taken together, these facts suggest that the actual initiation site may be the second ATG of human rather than the first. Exon 11 encodes the carboxyl-terminal domain as well as the entire 3′ untranslated region. Evidence exists demonstrating the presence of alternative 3′ polyadenylation sites in mouse ferrochelatase [15, 83] and discrimination between these sites appears to have something to do with erythroid versus non-erythroid cell expression [83].

The promoter region of human ferrochelatase has been examined in some detail by Brenner's group using both in vitro and in vivo approaches [84–86]. Their data reveal that a single ferrochelatase gene is regulated to provide housekeeping functions as well as erythroid-specific expression. The promoter region lacks both TATA and CAAT box motifs, but contains a CpG island in the region from -160 to $+400$ bp. Transient expression studies demonstrate that a minimal Sp1-driven promoter is sufficient for expression in non-erythroid cell lines and that a minimal promoter of -0.15 kb, which lacks both the GATA and NF-E2 elements, is sufficient to confer erythroid-specific expression. Interestingly, inclusion of the larger -4 kb promoter fragment which contains a number of putative erythroid-specifc elements failed to increase erythroid-specific expression over the level found with just the -0.15 kb fragment.

In transgenic mouse cell lines, however, maximal erythroid-specific induction occurred with the -4.0 kb region and this observation was proposed to reflect organized chromatin structure. In transgenic embryonic mouse cells, where a single copy of the reporter construct was inserted, developmentally specific expression was obtained with the human ferrochelatase promoter fragment containing the Sp1, NF-E2, and GATA elements. In vivo erythroid specificity is presumably mediated via GATA-1 and NF-E2 elements present around -300 bp along with additional erythroid-specific elements approximately -2 kb upstream from the transcriptional start site. Additionally, Asano et al. [87] have recently shown that FKLF-2, a novel Krüppel-like transcriptional factor, is also involved in activation of ferrochelatase transcription. Examination of murine ferrochelatase in differentiating MEL cells suggests a putative erythroid-specific element in the -80 to -72 region [88].

Recently, a role for HNF-1 alpha in regulation of mouse ferrochelatase has been suggested from studies with HNF-1 alpha-null mice [89]. Yet to be examined in detail are possible drug- or hormonal-responsive promoter elements whose existence is suggested by observed alterations in ferrochelatase activity following drug administration to whole animals [90].

Erythropoietic protoporphyria

In humans, a genetic defect that causes a reduction in ferrochelatase activity results in the disease erythropoietic protoporphyria (EPP) [19, 20]. In EPP, free protoporphyrin, mainly from erythropoietic tissues, is found to accumulate in the skin resulting in photosensitivity. While painful, this disease is generally not life threatening except in about 5% of individuals in whom the free protoporphyrin accumulates, crystallizes, and blocks biliary passages. In some cases, liver failure with cirrhosis may develop and without liver transplantation this condition is fatal.

While it has long been accepted that EPP in humans is a dominantly inherited disease, one most frequently finds only about 25% of normal enzyme activity in clinical EPP patients, compared to the 50% that would be anticipated and as found in other dominantly inherited porphyrias. Attempts to explain this observation have led to a variety of suggestions that include a third allele, a role of membrane lipids and diet, a dimeric

enzyme that only functions as a homodimer, and low expression of one allele. Recently, Gouya et al. [91] presented strong evidence in support of dominant inheritance with variant low-allele expression. Their data suggest that the inheritance of a single EPP ferrochelatase mutation is not sufficient to cause clinical EPP, but that the second ferrochelatase allele (which encodes a functional protein) must contain genomic elements in the 5′ region that cause low expression of the normal ferrochelatase mRNA. This model is attractive since it not only explains the low level of ferrochelatase activity, but may also help to explain the variable penetrance and variation of expression of EPP. However, their suggestion that an A-to-G polymorphism found in a majority of EPP patients contributes to the low expression has not been supported by work with transgenic mouse cells in which this genotype was recreated [86].

While the low-expression model is appealing and may explain some EPPs, the possibility that additional factors may be involved should not be entirely dismissed, especially in light of the considerable molecular heterogeneity that exists among the ferrochelatase genes of EPP patients. Since it is now clear that ferrochelatase is a homodimer and possesses a [2Fe-2S] cluster that is sensitive to NO in vivo and in vitro [72], the possibility exists that environmental and/or additional genetic factors may also play a role in modulating the level of ferrochelatase in vivo.

To date, over 30 different EPP mutations in human genomic ferrochelatase have been described, along with one partial chromosomal deletion [see ref. 92 and references therein]. Of the initial EPP mutation reports, one described by Nakahashi et al. [93] is now known to be not an EPP mutation, but a human polymorphism. Of the currently known mutations, there are 18 missense mutations and six different exon deletions (exons 3, 4, 5, 7, 9, and 10) (table 2). The positions of the known missense, non-termination mutations are shown on the crystal structure of human ferrochelatase in figure 6.

Table 2. Human erythropoietic protoporphyria mutations.

Missense mutations		Exon deletions of frameshifts	
G55C	T283I		
Q59X	M288I		
I71K	W301X		
R115X	S333P	1	7
S151P	P334L	3	8
I186T	V362G	4	9
Y191H	K379X	5	10
P192T	F417S		
M267I	ΔF417		

Compiled from Rufenacht et al. [92], Frank et al. [98], and references therein.

Interestingly, only two mutations, Y191H and P192T, are of residues that are located within the active site, with the remainder scattered throughout the protein. From a numerical standpoint, the largest number of patients have exon deletions. For many missense mutations, expression and assay of homodimeric recombinant protein has established that the mutation results in decreased levels of enzyme activity, and any exon deletion results in inactive enzyme [63]. However, a molecular explanation for the decrease in activity of most missense mutations is lacking since few studies have done more than measure enzyme activity, and none have examined the activity and physical properties of mixed dimers. Some mutations in ferrochelatase result in the enzyme not having an intact [2Fe-2S] cluster, and loss of this feature results in loss of enzyme activity.

Two different mouse models for EPP exist. One arose from whole-mouse chemical mutagenesis producing a missense mutation [94] that results in less than 10% residual activity in the homozygous mouse. The second EPP mouse was engineered to have an exon 10 deletion [95]. Interestingly, the heterozygous exon deletion mouse has 50% of normal ferrochelatase activity levels, unlike most symptomatic human EPPs, which lends credence to the suggestion that additional factors must be responsible for the normally observed 25% enzyme levels. Using a viral-vector-mediated transfer of wild-type ferrochelatase similar to that employed in cultured EPP cells [96], the homozygous EPP mouse model has recently been exploited in gene therapy experiments to correct the EPP photosensitivity phenotype [97].

Future directions

Over the past four decades, researchers have learned much about ferrochelatases, but much more remains to be explored. While the structures of two ferrochelatases are now known, the details of catalysis have yet to be fully described. Metallation involves porphyrin macrocycle distortion, but the mechanism whereby specific residues prompt this distortion is unknown. Suggestions for the participation of some residues in proton abstraction and metallation have been made, but the immediate source of iron, the fate of the two pyrrole protons, and the protoheme product are not known. This is an area that promises to move rapidly.

Understanding of the transcriptional regulation of mammalian ferrochelatase is advancing more rapidly than that for procaryotic and non-mammalian ferrochelatases. However, much remains to be determined in mammals to explain the diverse levels of ferrochelatase activity in different tissue types and the sensitivity of the gene to drugs and hormones. Plant ferrochelatases and ‘plant EPP’ have only recently gar-

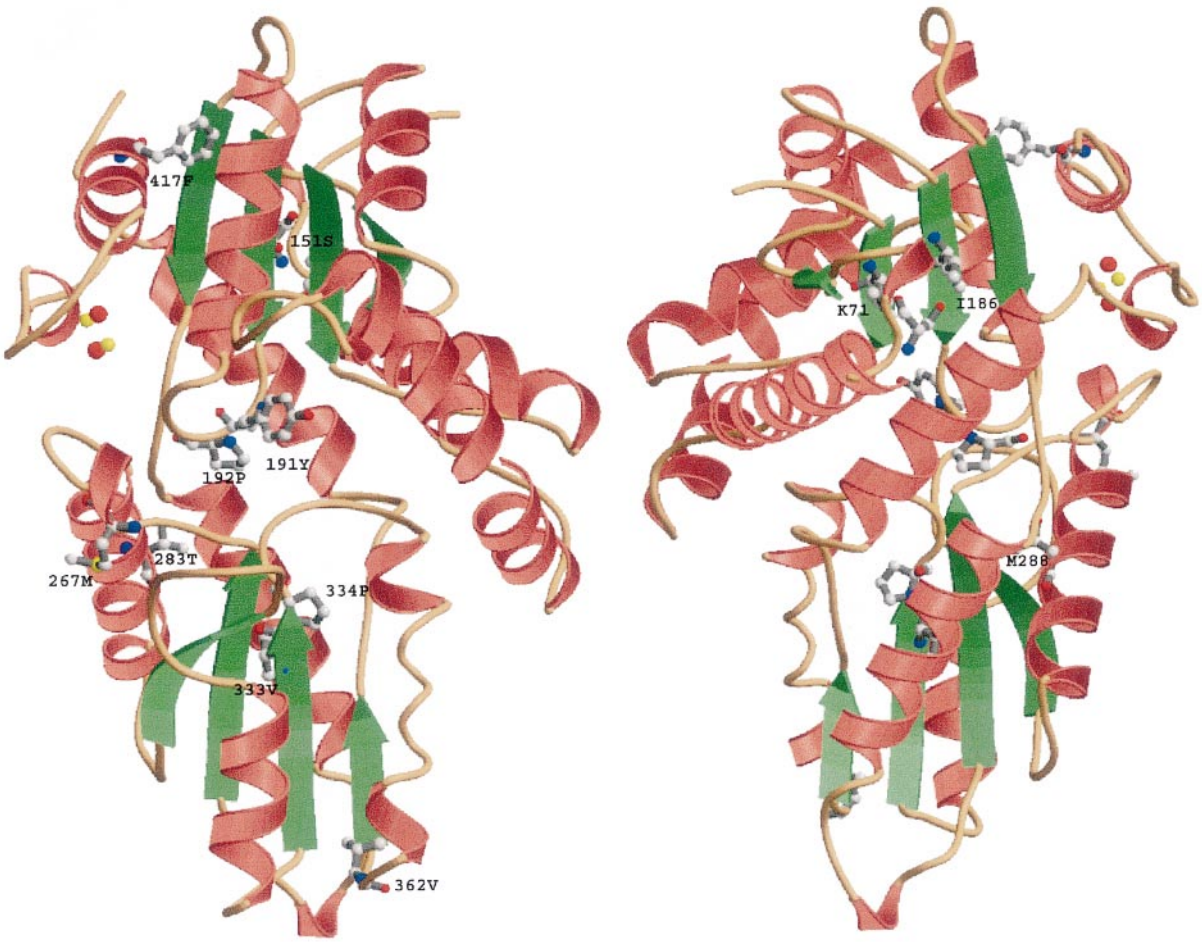

Figure 6. Location of human erythropoietic protoporphyria (EPP) mutations. A single monomer is shown front and back to demonstrate the position of residues that have been found modified in EPP patients.

nered the attention they deserve, and a rich variety of regulatory mechanisms will likely be found to exist in procaryotes. These promise to be exciting and fruitful fields for the next decade.

The potential biomedical importance of ferrochelatase other than in EPP is currently poorly explored, but even for EPP our knowledge is still rudimentary. Although advances have been made, we still do not have a clear understanding of the variably penetrant nature of EPP, nor do we even know if the diverse gene mutations all have equal probability to cause clinical manifestations of EPP. DNA microarray-based approaches should hold great promise to approach these interesting questions. Another area to be considered is the role that ferrochelatase may play as a target for photodynamic therapy of some cancers. To date, there is no satisfactory explanation for why ALA administration to tumor tissues results in the intracellular accumulation of protoporphyrins rather than heme or heme degradation products and this would seem to be a topic with potentially profound implications.

Acknowledgements. This work was supported by grant DK 32303 from the National Institutes of Health. We wish to acknowledge the many contributions from past members of this laboratory and collaborators.

1 Goldberg A., Ashenbrucker M., Cartwright G. E. and Wintrobel M. M. (1956) Studies on the biosynthesis of heme in vitro by avian erythrocytes. Blood **11:** 821–833
2 Jones O. T. G. (1968) Ferrochelatase of spinach chloroplasts. Biochem. J. **107:** 113–119
3 Jones M. S. and Jones O. T. G. (1970) Ferrochelatase of *Rhodopseudomonas spheroides*. Biochem. J. **119:** 453–462
4 Jones M. S. and Jones O. T. G. (1969) The structural organization of haem synthesis in rat liver mitochondria. Biochem. J. **113:** 507–514

5 Tokunaga R. and Sano S. (1972) Comparitive studies on nonenzymatic and enzymatic protoheme formation. Biochim. Biophys. Acta **264:** 263–271
6 Kassner R. J. and Walchak H. (1973) Heme formation from Fe(II) and porphyrin in the absence of ferrochelatase activity. Biochim. Biophys. Acta **304:** 294–303
7 Dailey H. A., Jr and Lascelles J. (1974) Ferrochelatase activity in wild-type and mutant strains of *Spirillum itersoni*: solubilization with chaotropic reagents. Arch. Biochem. Biophys. **160:** 523–529
8 Taketani S. and Tokunaga R. (1981) Rat liver ferrochelatase: purification, properties, and stimulation by fatty acids. J. Biol. Chem. **256:** 12748–12753
9 Dailey H. A. and Fleming J. E. (1983) Bovine ferrochelatase: kinetic analysis of inhibition by N-methylprotoporphyrin, managanese, and heme. J. Biol. Chem. **258:** 11453–11459
10 Taketani S. and Tokunaga R. (1982) Purification and substrate specificity of bovine liver-ferrochelatase. Eur. J. Biochem. **127:** 443–447
11 Camadro J. M. and Labbe P. (1988) Purification and properties of ferrochelatase from the yeast *Saccharomyces cerevisiae*: evidence for a precursor form of the protein. J. Biol. Chem. **263:** 11675–11682
12 Labbe-Bois R. (1990) The ferrochelatase from *Saccharomyces cerevisiae*: sequence, disruption, and expression of its structural gene HEM15. J. Bio1. Chem. **265:** 7278–7283
13 Taketani S., Inazawa J., Nakahashi Y., Abe T. and Tokunaga R. (1992) Structure of the human ferrochelatase gene: exon/intron gene organization and location of the gene to chromosome 18. Eur. J. Biochem. **205:** 217–222
14 Taketani S., Nakahashi Y., Osumi T. and Tokunaga R. (1990) Molecular cloning, sequencing, and expression of mouse ferrochelatase. J. Biol. Chem. **265:** 19377–19380
15 Brenner D. A. and Frasier F. (1991) Cloning of murine ferrochelatase. Proc. Natl. Acad. Sci. USA **88:** 538–849
16 Eldridge M. G. and Dailey H. A. (1992) Yeast ferrochelatase: expression in a baculovirus system and purification of the expression protein. Prot. Sci. **1:** 271–277
17 Brenner D. A., Didier J. M., Frasier F., Christensen S. R., Evans and Dailey H. A. (1992) A molecular defect in human protoporphyria. Am. J. Hum. Genet. **50:** 1203–1210
18 Dailey H. A., Sellers V. M. and Dailey T. A. (1994) Mammalian ferrochelatase: expression and characterization of normal and two human protoporphyric ferrochelatases. J. Biol. Chem. **269:** 390–395
19 Moore M. R., McColl K. E., Rimington C. and Goldberg A. (1987) Disorders of Porphyrin Metabolism, vol. 1, Plenum, New York
20 Nordmann Y. and Deybach J. C. (1990) Human hereditary porphyrias. In: Biosynthesis of Heme and Chlorophylls, pp. 491–542, Dailey H. A. (ed.), McGraw-Hill, New York
21 Dailey H. A. (1990) Conversion of coproporphyrinogen to protoheme in higher eukaryotes and bacteria. In: Biosynthesis of Heme and Chlorophylls, pp. 123–155, Dailey H. A. (ed.), McGraw-Hill, New York
22 Dailey H. A. (1996) Ferrochelatase. In: Mechanisms of Metallocenter Assembly, pp. 77–98, Hausinger R. P., Eichorn G. L. and Marzilli L. G. (eds), VCH, New York
23 Honeybourne C. L., Jackson J. T. and Jones O. T. G. (1979) The interaction of mitochondrial ferrochelatase with a range of porphyrin substrates. FEBS Lett. **98:** 207–210
24 Dailey H. A. (1982) Purification and characterization of membrane-bound ferrochelatase from *Rhodopseudomonas sphaeroides*. J. Biol. Chem. **257:** 14714–14718
25 Dailey H. A. and Smith A. (1984) Differential interaction of porphyrins used in photoradiation therapy with ferrochelatase. Biochem J. **223:** 441–445
26 Dailey H. A., Jones C. S. and Karr S. W. (1989) Interaction of free porphyrins and metalloporphyrins with mouse ferrochelatase: a model for the active site of ferrochelatase. Biochim. Biophys. Acta **999:** 7–11
27 Goldberg D. E. and Thomas K. M. (1976) Crystal and molecular structures of N-substituted porphyrin: chloro (2,3,7,12,13,17,18-octaethyl-N-ethylacetatoporphine) cobalt (II). J. Am. Chem. Soc. **98:** 913–919
28 Lavallee D. K. (1987) The Chemistry and Biochemistry of N-substituted Porphyrins, VCH, New York
29 Lavallee D. K. (1988) Porphyrin metallation reactions in biochemistry. In: Mechanistic Principles of Enzyme Activity, pp. 279–317, Liebman J. F. and Greenberg A. (eds), VCH, New York
30 De Matteis F., Gibbs A. H. and Smith A. G. (1980) Inhibition of protohaem ferro-lyase by N-substituted porphyrins: structural requirements for the inhibitory effect. Biochem. J. **189:** 645–648
31 Marks G. S., Allen D. T., Johnston C. T., Sutherland E. P., Nakatsu K. and Whitney R. A. (1985) Suicidal destruction of cytochrome P-450 and reduction of ferrochelatase activity by 3,5-diethoxycarbonyl-1, 4-dihydro-2,4-dihydro-2,4,6-trimethylpyridine and its analogues in chick embryo liver cells. Mol. Pharmacol. **27:** 459–465
32 Lecerof D., Fodje M., Hansson A., Hansson M. and Al-Karadaghi S. (2000) Structural and mechanistic basis of prophyrin metallation by ferrochelatase. J. Mol. Biol. **297:** 221–232
33 Gamble J. T., Dailey H. A. and Marks G. S. (2000) N-methylprotoporphyrin is a more potent inhibitor of recombinant human than of recombinant chicken ferrochelatase. Drug Metab. Dispos. **28:** 373–375
34 Dailey H. A. (1987) Metal inhibition of ferrochelatase. Ann. NY Acad. Sci. **514:** 81–86
35 Rossi E., Taketani S. and Garcia-Webb P. (1993) Lead and the terminal mitochondrial enzymes of haem biosynthesis. Biomed. Chromatogr. **7:** 1–6
36 Jaffe E. K. (2000) The porphobilinogen synthase family of metalloenzymes. Acta Cryst. **D56:** 115–128
37 Taketani S., Tanaka-Yoshioka A., Masaki R., Tashiro Y. and Tokunaga R. (1986) Association of ferrochelatase with complex I in bovine heart mitochondria. Biochim. Biophys. Acta **883:** 277–283
38 Porra R. J., Vitols K. S., Labbe R. F. and Newton N. A. (1967) Studies on ferrochelatase: the effects of thiols and other factors on the determination of activity. Biochem. J. **104:** 321–327
39 Porra R. J. and Lascelles J. (1968) Studies on ferrochelatase: the enzymic formation of haem in proplastids, chloroplasts and plant mitochondria. Biochem. J. **108:** 343–348
40 Punekar N. S. and Gokhale R. S. (1991) Factors influencing the stability of heme and ferrochelatase: role of oxygen. Biotechnol. Appl. Biochem. **14:** 21–29
41 Franco R., Moura J. J. G., Moura I., Lloyd S. G., Huynh B. H., Forbes W. S. et al. (1995) Characterization of the iron-binding site in mammalian ferrochelatase by kinetic and Mossbauer methods. J. Biol. Chem. **270:** 26352–26357
42 Debussche L., Coulder M., Thibaut D., Cameron B., Crouzet J. and Blanche F. (1992) Assay, purification, and charactrerization of cobaltochelatase, a unique enzyme complex catalyzing cobalt insertion in hydrogenbyrinic a,c-diamide during coenzyme B_{12} biosynthesis in *Pseudomonas denitrificans*. J. Bacteriol. **174:** 7445–7451
43 Warren M. J. and Scott A. L. (1990) Tetrapyrrole assembly and modification into the ligands of biologically functional cofactors. Trends Biochem. Sci. **12:** 486–491
44 Hambright P. (1975) Dynamic coordination chemistry of metalloporphyrins. In: Porphyrins and Metalloporphyrins, pp. 233–278, Smith K. (ed.), Elsevier, Amsterdam
45 Warren M. J., Bolt E. L., Roessner C. A., Scott A. I., Spencer J. B. and Woodcock S. C. (1994) Gene dissection demonstrates that the *Escherichia coli cysG* gene encodes a multifunctional protein. Biochem. J. **382:** 837–841
46 Ferreira G. C., Andrew T. L., Karr S. W. and Dailey H. A. (1988) Organization of the terminal two enzymes of the heme biosynthetic pathway: orientation of protoporphyrinogen oxidase and evidence for a membrane complex. J. Biol. Chem. **263:** 3835–3839

47 Proulx K. L., Woodard S. I. and Dailey H. A. (1993) In situ conversion of coproporphyrinogen to heme by murine mitochondria: terminal steps of the heme biosynthetic pathway. Prot. Sci. **2:** 1092–1098

48 Takeda J., Ohya T. and Sato M. (1992) Ferrochelatase transition-state model: rapid incorporation of copper (II) into nonplanar dodecaphenylporphyrin. Inorg. Chem. **31:** 2877–2880

49 Cochran A. G. and Schultz P. G. (1990) Antibody-catalyzed porphyrin metallation. Science **249:** 781–783

50 Li Y. and Sen D. (1997) Toward an efficient DNAzyme. Biochemistry **36:** 5589–5599

51 Morgan M., Prudent J. R. and Schultz P. G. (1996) Porphyrin metalation catalyzed by a small RNA molecule. J. Am. Chem. Soc. **118:** 7012–7013

52 Blackwood M. E., Jr, Rush T. S. III, Medlock A., Dailey H. A. and Spiro T. G. (1997) Resonance Raman spectra of ferrochelatase reveal porphyrin distortion upon metal binding. J. Am. Chem. Soc. **119:** 12170–12174

53 Blackwood M. E., Jr, Rush T. S. III, Romesberg F., Schultz P. G. and Spiro T. G. (1998) Alternative modes of substrate distortion in enzyme and antibody catalyzed ferrochelation reactions. Biochemistry **37:** 779–782

54 Franco, R., Ma, J.-G., Lu, Y., Ferreira, G. C., and Shelnutt, J. A. (in press) Porphyrin interactions with wild-type and mutant mouse ferrochelatase. Biochemistry

55 Karr S. R. and Dailey H. A. (1988) The synthesis of murine ferrochelatase in vitro and in vivo. Biochem. J. **254:** 799–803

56 Chow K. S., Singh D. P., Walker A. R. and Smith A. G. (1998) Two different genes encode ferrochelatase in *Arabidopsis*: mapping, expression and subcellular targeting of the precursor proteins. Plant J. **15:** 531–541

57 Suzuki T., Masuda T., Inokuchi H., Shimada H., Ohata H. and Takamiya T. (2000) Overexpresxion, enzymatic properties and tissue localization of a ferrochelatase of cucumber. Plant Cell Physiol. **41:** 192–199

58 Harbin B. M. and Dailey H. A. (1985) Orientation of ferrochelatase in bovine liver mitochondria. Biochemistry **24:** 366–370

59 Wu, C.-K., Dailey, H. A., Rose, J. P., Burden, A. M., and Wang, B.-C. (in press) The 2Å structure of human ferrochelatase, the terminal enzyme of heme biosynthesis. Nat. Struct. Biol

60 Straka J. G., Bloomer J. R. and Kempner E. S. (1991) The functional size of ferrochelatase determined in situ by radiation inactivation. J. Biol. Chem. **266:** 24637–24641

61 Burden A. E., Wu C.-K., Dailey T. A., Busch J. L. H., Dhawan I. K., Rose J. P. et al. (1999) Human ferrochelatase: crystallization, characterization of the [2Fe-2S] cluster and determination that the enzyme is a homodimer. Biochim. Biophys. Acta **1435:** 191–197

62 Al-Karadaghi S., Hansson M., Nikonov S., Jonsson B. and Hederstedt L. (1997) Crystal structure of ferrochelatase: the terminal enzyme in heme biosynthesis. Structure **5:** 1501–1510

63 Sellers V. M., Dailey T. A. and Dailey H. A. (1998) Examination of ferrochelatase mutations that cause erythropoietic protoporphyria. Blood **91:** 3980–3985

64 Dailey H. A. (1985) Spectroscopic examination of the active site of bovine ferrochelatase. Biochemistry **24:** 1287–1291

65 Dailey H. A. and Fleming J. E. (1986) The role of arginyl residues in porphyrin binding to ferrochelatase. J. Biol. Chem. **261:** 7902–7905

66 Gora M., Rytka J. and Labb-Bois R. (1999) Activity and cellular location in *Saccharomyces cerevisiae* of chimeric mouse/yeast and Bacillus subtilis/yeast ferrochelatases. Arch. Biochem. Biophys. **361:** 231–240

67 Dailey H. A., Finnegan M. G. and Johnson M. K. (1994) Human ferrochelatase is an iron-sulfur protein. Biochemistry **3:** 403–407

68 Ferreira G. C., Franco R., Lloyd S. G., Pereira A. S., Moura I., Moura J. J. G. et al. (1994) Mammalian ferrochelatase, a new addition to the metalloenzyme family. J. Biol. Chem. **269:** 7062–7065

69 Day A. L., Parsons B. M. and Dailey H. A. (1998) Cloning and characterization of *Gallus* and *Xenopus* ferrochelatases: presence of the [2Fe-2S] cluster in nonmammalian ferrochelatase. Arch. Biochem. Biophys. **359:** 160–169

70 Sellers V. M., Wang K.-F., Johnson M. K. and Dailey H. A. (1998) Evidence that the fourth ligand to the [2Fe-2S] cluster in animal ferrochelatase is a cysteine: characterization of the enzyme from *Drosophila melanogaster*. J. Biol. Chem. **273:** 22311–22316

71 Crouse B. R., Sellers V. M., Finnegan M. G., Dailey H. A. and Johnson M. K. (1996) Site-directed mutagenesis and spectroscopic characterization of human ferrochelatase: identification of residues coordinating the [2Fe-2S] cluster. Biochemistry **35:** 16222–16229

72 Sellers V. M., Johnson M. K. and Dailey H. A. (1996) Function of the [2Fe-2S] cluster in mammalian ferrochelatase: a possible role as a nitric oxide sensor. Biochemistry **35:** 2699–2704

73 Medlock A. E. and Dailey H. A. (2000) Examination of the carboxyl-terminal chimeric constructs of human and yeast ferrochelatases. Biochemistry **39:** 7461–7467

74 Kirkman H. N., Rolfo M., Ferraris A. M. and Gaetani G. F. (1999) Mechanisms of protection of catalase by NADPH: kinetics and stoichiometry. J. Biol. Chem. **274:** 13908–13914

75 Kohno H., Okuda M., Furukawa T., Tokunaka R. and Taketani S. (1994) Site-directed mutagenesis of human ferrochelatase: identification of histidine-263 as a binding site for metal ions. Biochim. Biophys. Acta **1209:** 95–100

76 Gora M., Grzybowska E., Rytka J. and Labbe-Bois R. (1996) Probing the active-site residues in *Saccharomyces cerevisiae* ferrochelatase by directed mutagenesis: in vivo and in vivo analyses. J. Biol. Chem. **271:** 11810–11816

77 Labbe-Bois R. and Camabro J.-M. (1994) Ferrochelatase in *Saccharomyces cerevisiae*. In: Metal Ions in Fungi, pp. 413–453, Winkelmann G. and Winge D. R. (eds), Dekker, New York

78 Luecke H., Schobert B., Richter H.-T., Cartailler J.-P. and Lanyi J. K. (1999) Structural changes in bacteriorthodopsin during ion transport at 2 angstrom resolution. Science **286:** 255–260

79 Adelroth P., Ek M. S., Mitchell D. M., Gennis R. B. and Brzezinski P. (1997) Glutamate 286 in cytochrome aa3 from *Rhodobacter sphaeroides* is involved in proton uptake during the reaction of the fully-reduced enzyme with dixoygen. Biochemistry **36:** 13824–13829

80 Schubert H. L., Raux E., Wilson K. S. and Warren M. J. (1999) Common chelatase design in the branched tetrapyrrole pathways of heme and anaerobic cobalamin synthesis. Biochemistry **38:** 10660–10669

81 Lange H., Kispal G. and Lill R. (1999) Mechanism of iron transport to the site of heme synthesis inside yeast mitochondria. J. Biol. Chem. **274:** 18989–18996

82 Whitcombe D. M., Carter N. P., Albertson D. G., Smith S. J., Rhodes D. A. and Cox T. M. (1991) Assignment of the human ferrochelatase gene (FECH) and a locus for protoporphyria to chromosome 18q22. Genomics **11:** 1152–1154

83 Chan R. Y., Schulman H. M. and Ponka P. (1993) Expression of ferrochelatase mRNA in erythroid and non-erythroid cells. Biochem. J. **292:** 343–349

84 Tugores A., Magness S. T. and Brenner D. A. (1994) A single promoter directs both housekeeping and erythroid preferential expression of the human ferrochelatase gene. J. Biol. Chem. **269:** 30789–30797

85 Magness S. T., Tugores A., Diala E. S. and Brenner D. A. (1998) Analysis of the human ferrochelatase promoter in transgenic mice. Blood **92:** 320–328

86 Magnus S. T., Tugores A. and Brenner D. A. (2000) Analysis of ferrochelatase expression during hematopoietic development of embryonic stem cells. Blood **95:** 3568–3577

87 Asano H., Li X. S. and Stamatoyannopoulos G. (2000) FKLF-2: a novel Krüppel-like transcriptional factor that activates globin and other erythroid lineage genes. Blood **95:** 3578–3584

88 Taketani S., Mohri T., Hioki K., Tokunaga R. and Kohno H. (1999) Structure and regulation of the mouse ferrochelatase gene. Gene **227:** 117–124
89 Muppala V., Lin C. S. and Lee Y. H. (2000) The role of HNF-1 alpha in controlling hepatic catalase activity. Mol. Pharmacol. **57:** 93–100
90 Tephly T. R., Hasegawa E. and Baron J. (1971) Effects of durgs on heme synthesis in the liver. Metabolism **20:** 200–214
91 Gouya L., Puy H., Lamoril J., Da Silva V., Grandchamp B., Nordmann Y. et al. (1999) Inheritance in erythropoietic protoporphyria: a common wild-type ferrochelatase allelic variant with low expression accounts for clinical manifestation. Blood **93:** 2105–2110
92 Rufenacht U. B., Gouya L., Schneider-Yin X., Puy H., Schafer B. W., Aquaron R. et al. (1998) Systematic analysis of molecular defects in the ferrochelatase gene from patients with erythropoietic protoporphyria. Am. J. Hum. Genet. **62:** 1341–1352
93 Nakahashi Y., Fujiti H., Taketani S., Ishida N., Kappas A. and Sassa S. (1992) The molecular defect of ferrochelatase in a patient with erythropoietic protoporphyria. Proc. Natl. Acad. Sci. USA **89:** 281–285
94 Boulechfar S., Lamoril J., Montagutelli X., Guenet J. L., Deybach J. C., Nordmann Y. et al. (1993) Ferrochelatase structural mutant (Fechml Pas) in the house mouse. Genomics **16:** 645–648
95 Magness S. T. and Brenner D. A. (1999) Targeted disruption of the mouse ferrochelatase gene producing an exon 10 deletion. Biochim. Biophys. Acta **1453:** 161–174
96 Magness S. T. and Brenner D. A. (1995) Ferrochelatase cDNA delivered by adenoviral vector corrects biochemical defect in protoporphyric cells. Hum. Gene Ther. **6:** 1285–1290
97 Pawliuk R., Bachelot T., Wise R. J., Mathews-Roth M. M. and Leboulch P. (1999) Long-term cure of the photosensitivity of murine erythropoietic protoporphyria by preselective gene therapy. Nat. Med. **5:** 768–773
98 Frank J., Nelson J., Wang X., Yang L., Ahmed W., Lam H. et al. (1999) Erthropoietic protoporphyria: identification of novel mutations in the ferrochelatase gene and comparison of biochemical markers versus molecular analysis as diagonistic strategies. J. Invest. Med. **47:** 278–284